Supplementary information for

Single-cell biophysical study reveals deformability and internal ordering relationship in T cells

Blanca González-Bermúdez,[1,2] Hikaru Kobayashi,[3] Álvaro Navarrete,[4] César Nyblad,[1,2] Mónica González-Sánchez,[3] Mónica de la Fuente,[3] Gonzalo Fuentes,[2,5] Gustavo V. Guinea,[1,2,6] Claudio García[4], Gustavo R. Plaza[1,2*]

[1] Center for Biomedical Technology. Universidad Politécnica de Madrid, E-28223 Pozuelo de Alarcón, Spain.
[2] Departamento de Ciencia de Materiales, ETSI de Caminos, Canales y Puertos. Universidad Politécnica de Madrid, E-28040 Madrid, Spain.
[3] Departamento de Genética, Fisiología y Microbiología. Facultad de Ciencias Biológicas. Universidad Complutense de Madrid. E-28040 Madrid, Spain.
[4] Departamento de Ingeniería Mecánica. Universidad de Santiago de Chile. Chile.
[5] Instituto de Sistemas Optoelectrónicos y Microtecnología. Universidad Politécnica de Madrid, E-28040 Madrid, Spain.
[6] Biomedical Research Networking Center in Bioengineering, Biomaterials and Nanomedicine (CIBER-BBN), Madrid, Spain.
*corresponding author: gustavo.plaza@upm.es

The supplementary information of this article consists of (a) five supplementary figures included in the next pages, (b) a supplementary table included in the next pages and six supplementary tables provided in an .xlsx spreadsheet file, (c) five supplementary videos in separate .avi files. The descriptions of the supplementary tables and supplementary videos are given in the final part of this document.

Supplementary Figures

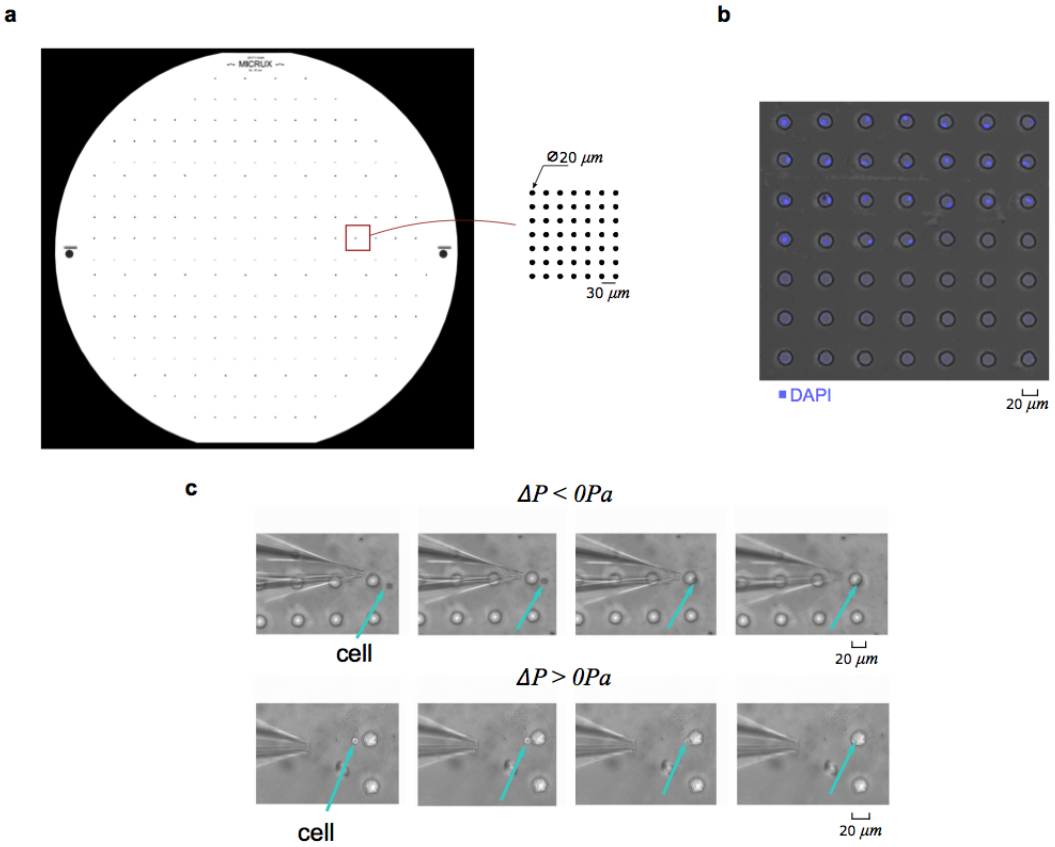

Supplementary Fig. 1. Microdeposition device for single-cell aspiration, deposition and imaging of cells. a, CAD layout of the single-cell microarray mold. The microarray platform was made from PDMS, containing 7x7 cylindrical microwells of 8-20 μm in diameter, 15 μm in height. In this work, arrays of microwells of 20 μm in diameter were used. **b**, Superimposed light and fluorescence microscopic image of single memory $CD4^+$ T cells on a microarray device after aspiration and immunostaining. **c**, Representative approaches for single-cell release and confinement in microwells after aspiration. Cells were placed into microwells by the application of a negative (upper panel) or positive (lower panel) differential pressure or on the tip of the pipette.

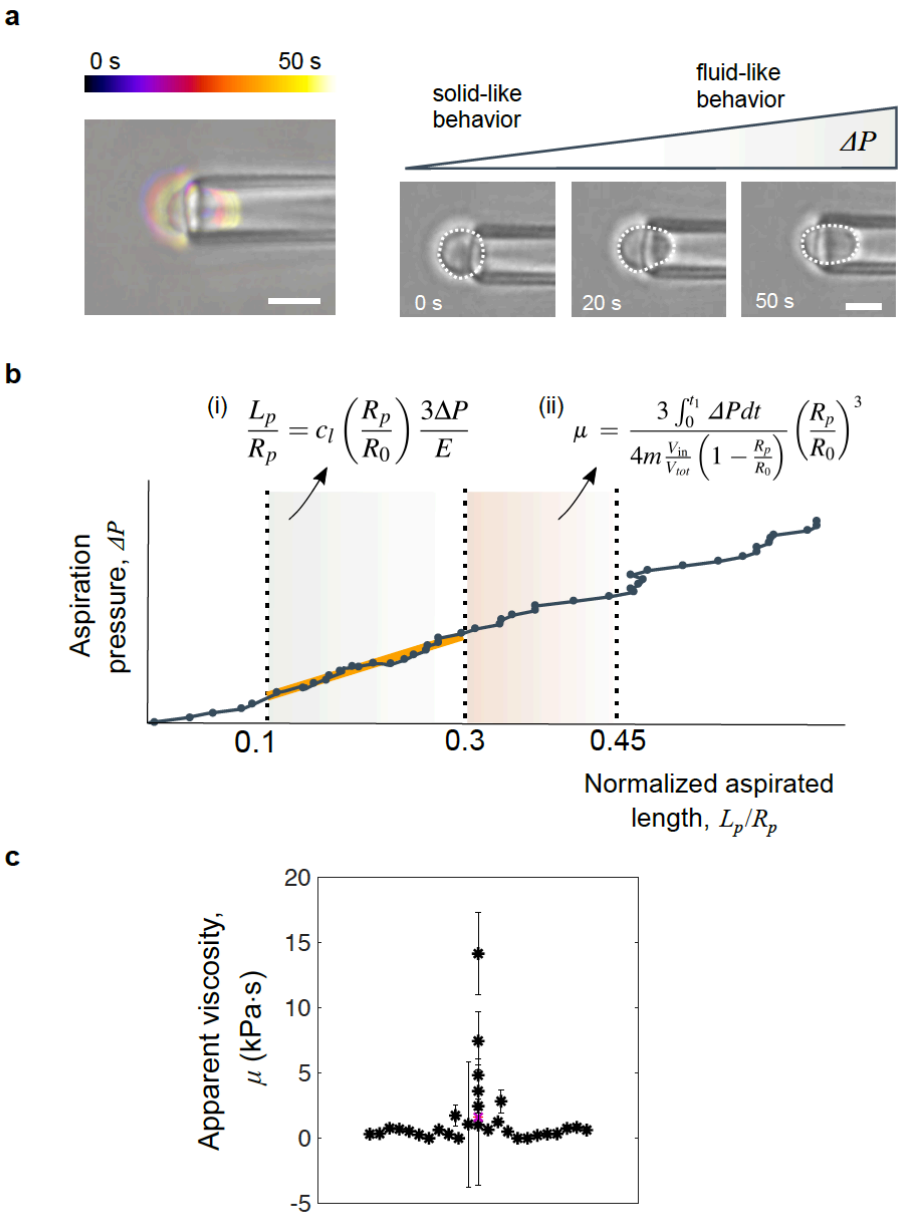

Supplementary Fig. 2. Analysis of the mechanical tests using micropipette aspiration. a, Bright-field image sequence of a representative micropipette-aspiration test. The dashed line indicates the contour of a cell undergoing aspiration. On the upper part, we show the applied ramp of differential pressure to aspirate cells. For small strains, cells display a solid-like behavior, while for large strains a fluid-like behavior can be observed; scale bar: 5 μm, rate of aspiration pressure: 5 Pa/s. **b**, Normalized aspirated length-aspiration pressure relation for a given cell. Inset: (i) equation to determine the apparent elastic modulus of the cell E, computed in the range region $0.1<L_p/R_p<0.3$[22]; (ii) equation to determine the apparent viscosity of the cell, μ, computed in the range region $0.3<Lp/Rp<0.45$[38]. **c**, Experimental apparent viscosity of cells. Each point corresponds to the mean of the apparent viscosity calculated within the range $0.3<L_p/R_p<0.45$; mean ± std. error, analyzed cells = 27, number of mice = 3.

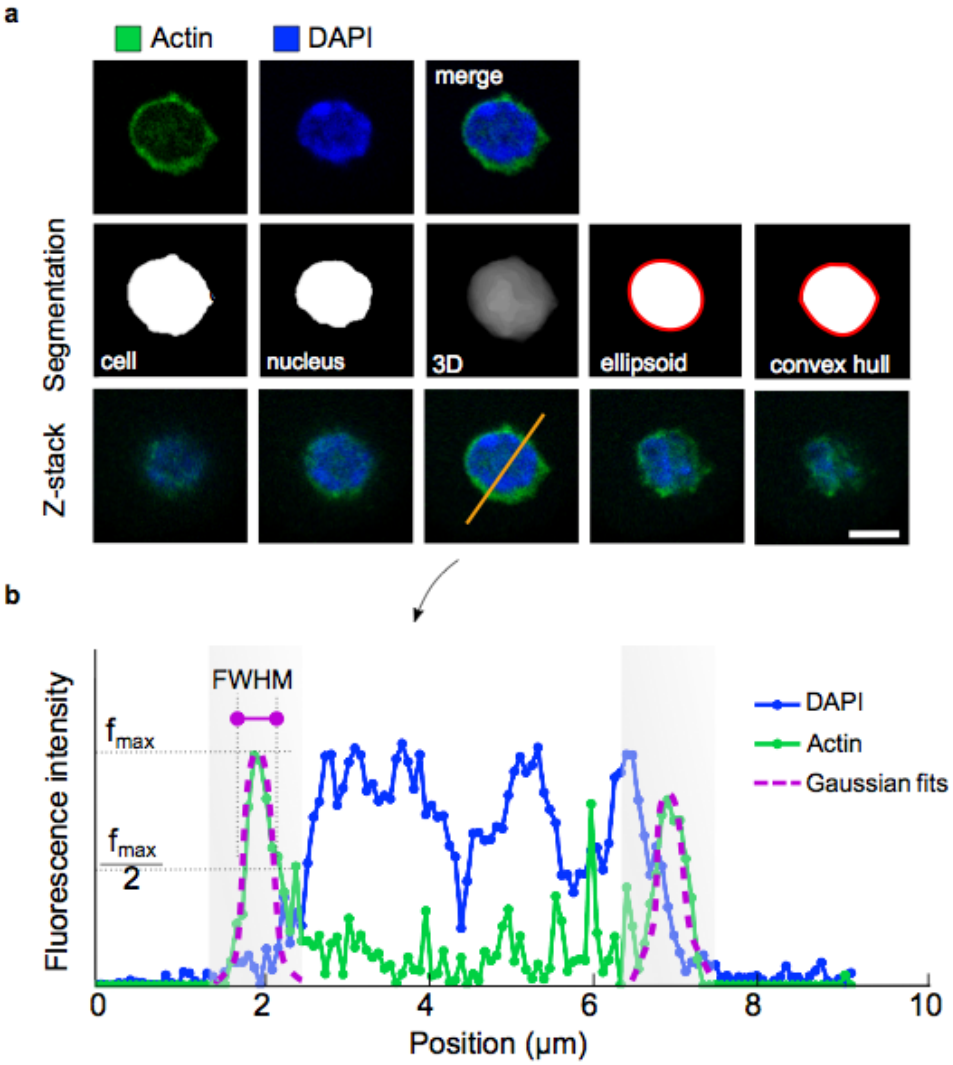

Supplementary Fig. 3. **3D analyses of actin cortex, nuclear and cellular geometry of memory CD4$^+$ T cells**. **a**, Upper panel: representative confocal images of a memory CD4$^+$ T cell, staining on actin (green) and DAPI (blue), at the equatorial plane. Middle panel: segmented images serve to perform a 3D reconstruction of the nucleus and the whole cell. To estimate volumetric and shape features, the 3D reconstructions are fitted using both an ellipsoid and a convex-hull approach (see Supplementary Tables 1-3 for details on the geometrical parameters). Lower panel: z-stack of confocal images, from apical (left) to basal (right) planes. Scale bar is 5 μm. **b**, Fluorescence intensity along 4 randomly oriented lines at equatorial plane (illustrated in the z-stack of A) were used to determine the thickness of the actin cytoskeleton. For each peak, as shown in the shaded regions, the actin intensity profile is fitted into a Gaussian function to compute the full width at half maximum (FWHM)

a

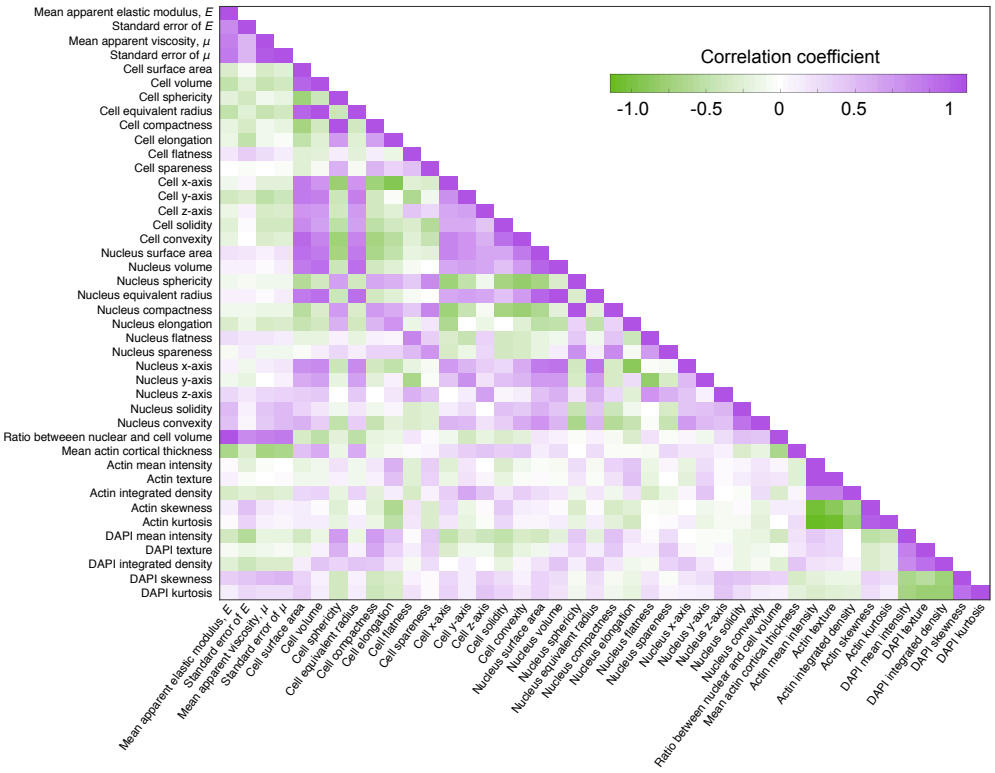
Correlation coefficient
-1.0
-0.5
0
0.5
1
Mean apparent elastic modulus, E
Standard error of E
Mean apparent viscosity, μ
Standard error of μ
Cell surface area
Cell volume
Cell sphericity
Cell equivalent radius
Cell compactness
Cell elongation
Cell flatness
Cell spareness
Cell x-axis
Cell y-axis
Cell z-axis
Cell solidity
Cell convexity
Nucleus surface area
Nucleus volume
Nucleus sphericity
Nucleus equivalent radius
Nucleus compactness
Nucleus elongation
Nucleus flatness
Nucleus spareness
Nucleus x-axis
Nucleus y-axis
Nucleus z-axis
Nucleus solidity
Nucleus convexity
Ratio betweeen nuclear and cell volume
Mean actin cortical thickness
Actin mean intensity
Actin texture
Actin integrated density
Actin skewness
Actin kurtosis
DAPI mean intensity
DAPI texture
DAPI integrated density
DAPI skewness
DAPI kurtosis

b

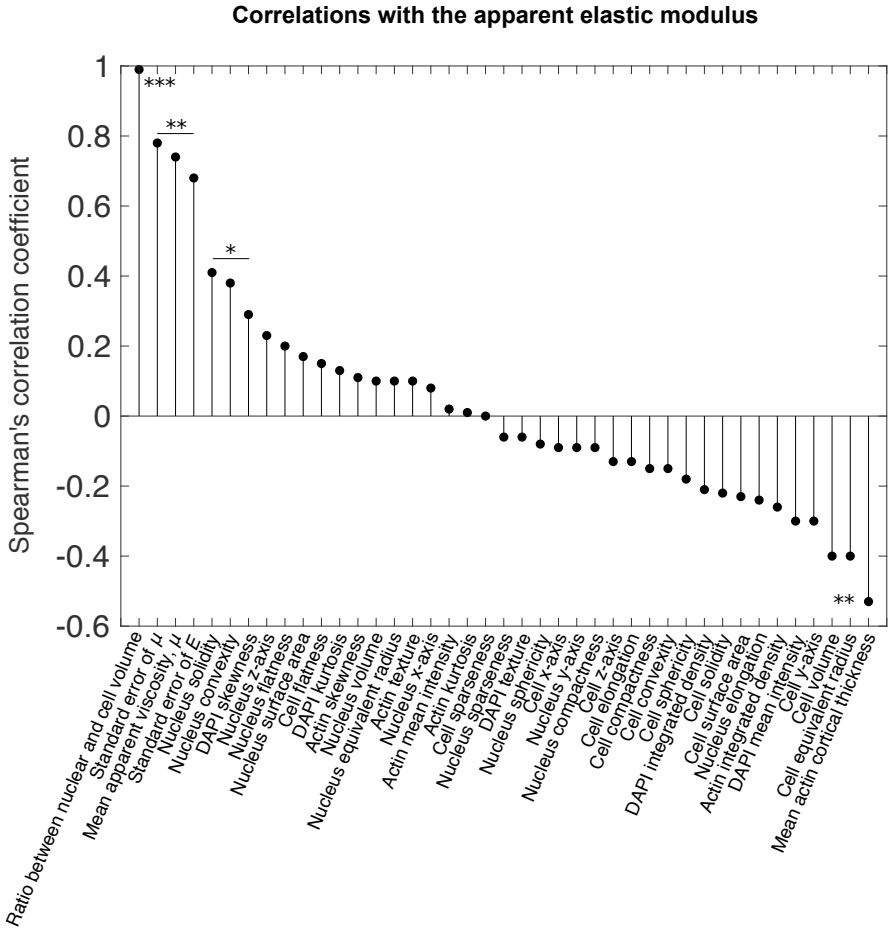
Correlations with the apparent elastic modulus
Spearman's correlation coefficient
1
0.8
0.6
0.4
0.2
0
-0.2
-0.4
-0.6
***
**
*
**
Ratio betweeen nuclear and cell volume
Standard error of μ
Mean apparent viscosity, μ
Standard error of E
Nucleus solidity
Nucleus convexity
DAPI skewness
Nucleus z-axis
Nucleus flatness
Nucleus surface area
Cell flatness
DAPI kurtosis
Actin skewness
Nucleus volume
Nucleus equivalent radius
Actin texture
Nucleus x-axis
Actin mean intensity
Actin kurtosis
Cell sparseness
Nucleus sparseness
DAPI texture
Nucleus sphericity
Cell x-axis
Nucleus y-axis
Nucleus compactness
Cell z-axis
Cell elongation
Cell compactness
Cell convexity
Cell sphericity
DAPI integrated density
Cell solidity
Cell surface area
Nucleus elongation
Actin integrated density
DAPI mean intensity
Cell y-axis
Cell volume
Cell equivalent radius
Mean actin cortical thickness

Supplementary Fig. 4. Heatmap of the Spearman's correlation coefficient between mechanical properties and 3D composition features. **a,** The 4 mechanical parameters include the average apparent elastic modulus (assuming a solid-like behavior, for small cell strains), the average apparent viscosity (fluid-like behavior, for large cell strains), and the standard errors of the means. The 3D composition features include 27 morphological measurements of cell and nucleus geometry and 11 biomolecular measurements of actin and DAPI content; green indicates a negative correlation, purple a positive correlation. **b,** Spearman's rank correlation coefficients (□) to assess the influence of morphological and biomolecular parameters on the apparent elastic modulus of memory $CD4^+$ T single-cells (***$p < 0.001$, **$p < 0.01$, *$p < 0.05$, being p the provability value associated with the Spearman rank correlation).

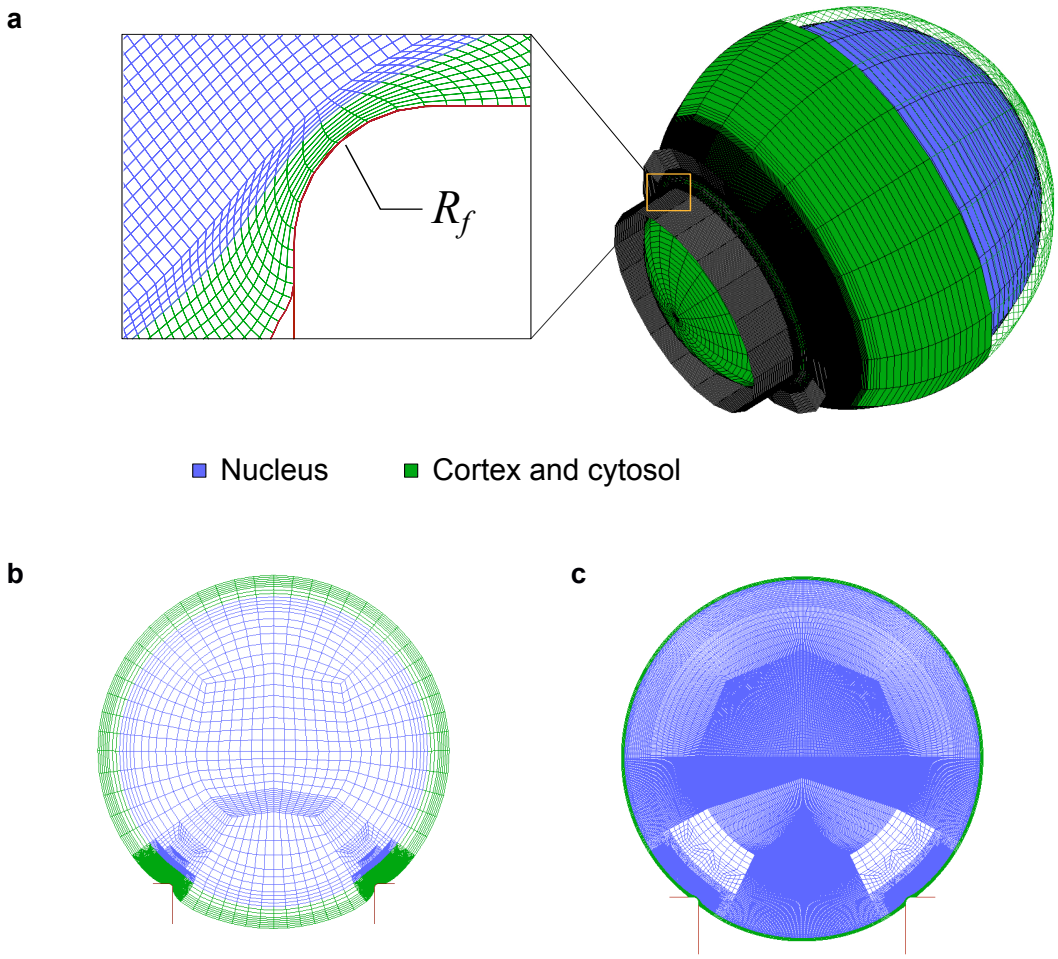

Supplementary Fig. 5. Two-layer finite-element model of micropipette-aspiration experiments of suspended cells. a, Snapshot of a 3D simulation of a cell undergoing aspiration (see Supplementary Video 3); **b**, Snapshot of a cell with R_n/R_c=0.83 being aspirated through a micropipette (see Supplementary Video 4). **c**, Snapshot of a cell with R_n/R_c=0.995 being aspirated through a micropipette (see Supplementary Video 5) ; cell nucleus is plotted in blue, the actin cortex in green and the micropipette in gray.

Supplementary Tables

Parameter	Unit	Description
Surface area	μm^2	Number of voxels at the border of each segmented object, computed using a discretized version of the Crofton formula.
Volume	μm^3	Number of voxels comprising the object, multiplied by the volume of an individual voxel-
Equivalent radius	μm	Equivalent radius of the object corresponding to the radius of a sphere.
Compactness	a.u.	Ratio of the squared object volume over the cube of the surface area, normalized such that the value for a sphere equals one: Compactness=$36\pi(\text{Volume})^2/(\text{Surface area})^3$
Sphericity	a.u.	Sphericity= Compactness $^{1/3}$
Elongation	a.u.	Ratio between the intermediate and longest semi-axis of the volume of the best fitted ellipsoid.
Flatness	a.u.	Ratio between the shortest and intermediate semi-axis of the volume of the best fitted ellipsoid.
Sparseness	a.u.	Ratio between the volume of the segmented object and the volume of the best fitted ellipsoid.
X-axis	μm	Scalar that specifies the length of the longest semi-axis of the ellipsoid that has the same normalized 3D moments as the segmented object.
Y-axis	μm	Scalar that specifies the length of the intermediate semi-axis of the ellipsoid that has the same normalized 3D moments as the segmented object.
Z-axis	μm	Scalar that specifies the length of the shortest semi-axis of the ellipsoid that has the same normalized 3D moments as the segmented object..
Solidity	a.u.	Ratio of voxels that are in the convex hull that are also in the segmented object: Solidity =Volume / Convex Volume
Convexity	a.u.	Ratio of surface pixels that are in the convex hull that are also in the segmented object: Convexity=Convex Surface Area/ Surface Area
Ratio between nuclear and cell volume	a.u.	Ratio between the equivalent spherical diameter of the nucleus and cell corresponding to the volume of spheres.
Mean intensity	a.u.	Mean intensity of voxel intensity of biomolecule content per segmented object.
Texture	a.u.	Standard deviation of voxel intensity of biomolecule content per segmented object.
Integrated density	a.u.	Product of the mean intensity of biomolecule content per segmented object and volume.
Skewness	a.u.	Skewness in the distribution of voxel intensities of biomolecule content per object.
Kurtosis	a.u.	Kurtosis in the distribution of voxel intensities of biomolecule content per object.
Actin cortical thickness	μm	Average FWHM of 8 fluorescence intensity profiles gaussian fits per cell (FWHM is the width of the actin signal at the point of half peak intensity).

Supplementary Table 1. **List, description and calculation of 3D morphological parameters.** Summary of 3D shape-based descriptors and 3D intensity-based descriptors used through-out the article.

The provided spreadsheet contains tables with data and experimental and numerical procedures. In **Supplementary Table 2**, we list software packages and references used in the confocal image analysis, and the steps of the workflow to analyze the confocal z-stack images are provided in **Supplementary Table 3**. In **Supplementary Table 4**, the full biomechanical parameters data are provided. In **Supplementary Table 5** the complete Spearman's correlation matrix is available, and the associated p-values can be found in in **Supplementary Table 6.** In **Supplementary Table 7** the numerical and geometrical parameters used in the simulations are indicated.

Supplementary Videos

Supplementary Video 1. Representative cell deposition in a microwell after micropipette aspiration, using a negative differential pressure (related to Supplementary Fig. 1c) to isolate the cell and continue the preparation of immunoassays. Scale bar is 20 μm.

Supplementary Video 2. Representative cell deposition in a microwell after micropipette aspiration, using a negative differential pressure (related to Supplementary Fig. 1d) to isolate the cell and continue the preparation of immunoassays. Scale bar is 20 μm.

Supplementary Video 3. Movie showing the results of the numerical simulation for R_n/R_c=0.83, extrapolated for a 3D visualization (related to Fig. 4). Cell nucleus is plotted in blue, the actin cortex in green and the micropipette in gray.

Supplementary Video 4. A cell with R_n/R_c=0.83 being aspirated through a micropipette under a differential pressure rate of 5.5 Pa/s. Cell nucleus is plotted in blue, the actin cortex in green and the micropipette in gray. Only the plane perpendicular to the axis of rotation is plotted for clarity.

Supplementary Video 5. A cell with R_n/R_c=0.995 being aspirated through a micropipette under a differential pressure rate of 7.5 Pa/s. Cell nucleus is plotted in blue, the actin cortex in green and the micropipette in gray. Only the plane perpendicular to the axis of rotation is plotted for clarity.